

Kinetic helicity, magnetic helicity and fast dynamo action

David W. Hughes^a, Fausto Cattaneo^b, Eun-jin Kim^a

^a Department of Applied Mathematical Studies, University of Leeds, Leeds LS2 9JT, UK

^b Department of Astronomy and Astrophysics, University of Chicago, Chicago, IL 60637, USA

Received 10 July 1996; revised manuscript received 24 September 1996; accepted for publication 26 September 1996

Communicated by A.P. Fordy

Abstract

The influence of the flow helicity on kinematic fast dynamo action is considered. Three different flows are studied, possessing identical chaotic properties but very different distributions of helicity (maximal helicity, zero net helicity and zero helicity density). All three flows provide strong evidence of fast dynamo action, indicating that helicity is not a crucial feature of fast dynamo flows. Comparisons are made between the magnetic fields generated by the three flows and it is established how certain key quantities scale with the magnetic Reynolds number. In particular, it is shown that the relative magnetic helicity tends to zero as the magnetic Reynolds number tends to infinity.

Cosmic magnetic fields are believed to be generated by the inductive motion of highly conducting fluids – dynamo action. In the simplest (kinematic) form of the dynamo problem the magnetic field \mathbf{B} and fluid velocity \mathbf{u} are related solely through the (dimensionless) induction equation

$$\partial_t \mathbf{B} = \nabla \times (\mathbf{u} \times \mathbf{B}) + R_m^{-1} \nabla^2 \mathbf{B}, \quad (1)$$

where R_m is the magnetic Reynolds number. The aim of kinematic dynamo theory is then to seek velocity fields that lead to the exponential growth of the magnetic energy density $\langle \mathbf{B}^2/2 \rangle$, where the average is taken over the volume of fluid V . It is useful to distinguish between two general types of dynamos; large scale (mean field) dynamos, in which the magnetic field has a scale of variation much larger than the velocity correlation length ℓ , and small scale dynamos in which the magnetic field varies on scales comparable with or smaller than ℓ . It is well known that a necessary condition for large scale dynamo action is that the underlying velocity field lacks reflectional symmetry,

i.e. it has a definite handedness [1]. One of the most natural measures of the lack of reflectional symmetry is the (kinetic or flow) *helicity*, defined by

$$\mathcal{H} = \int_V h \, d\mathbf{x}^3, \quad (2)$$

where $h = \mathbf{u} \cdot \nabla \times \mathbf{u}$ is the helicity density. Indeed, typically there is a strong relationship between the α -effect of mean field electrodynamics (responsible for mean field regeneration) and the flow helicity (although it is possible to have an α -effect with no helicity [2]). Helicity is generated naturally in rotating systems and, for this reason, all models of planetary, stellar and galactic dynamos have been based on helical flows. The handedness of the resulting large scale magnetic field is then determined by the handedness of the underlying turbulent flow; again this lack of reflectional symmetry is often manifested by non-zero *magnetic helicity*, defined by

$$\mathcal{H}_B = \int_V h_B \, d\mathbf{x}^3, \quad (3)$$

where $h_B = \mathbf{A} \cdot \nabla \times \mathbf{A}$, with $\mathbf{B} = \nabla \times \mathbf{A}$. An interpretation of this quantity in terms of linkages of magnetic field lines has been provided by Moffatt [3].

In the case of small scale dynamos the interesting question concerns the possibility of dynamo action in the limit of vanishing magnetic diffusivity (i.e. $R_m \rightarrow \infty$) – so-called *fast* dynamo action. It is well known that a necessary (though not sufficient) condition for fast dynamo action is that the flow be chaotic (i.e. has positive topological entropy). For flows that are steady solutions of the incompressible Euler equation this can be achieved only if the flow has the Beltrami property, $\nabla \times \mathbf{u} = \lambda \mathbf{u}$ with λ constant [4]. Obviously such flows are maximally helical. However, in general, the relation between the kinetic helicity of the underlying flow, small scale dynamo action and the magnetic helicity of the generated field is not at all well understood. In this letter we address these issues by considering three specific flows. They are related in that they have identical chaotic properties – measured, for example, by their Lyapunov exponents – but they differ markedly in their helicity distributions. In addition the flows are chosen all to possess the same kinetic energy.

We consider incompressible flows of the form

$$\mathbf{u}(x, y, t) = (\partial_y \psi, -\partial_x \psi, w), \quad \partial_z \psi = \partial_z w = 0. \quad (4)$$

With such velocities the induction equation supports solutions of the form

$$\mathbf{B}(x, t) = \hat{\mathbf{B}}(x, y, t) \exp(ikz), \quad (5)$$

and hence, for a fixed k , the resulting problem for the magnetic field is two-dimensional. Consequently, (1) can be solved numerically for quite large values of R_m ($O(10^3)$) without undue difficulty, thus facilitating the numerical investigation of fast dynamo action [5–8].

Fast dynamo action may be regarded as a competition between the exponential stretching of the magnetic field lines on the one hand and the effects of diffusion on the other. For flows of the form (4) exponential stretching takes place solely in the x - y plane, independently of w . The influence of w is felt only

in the folding of the magnetic field; this may be constructive, thus generating significant magnetic flux, or destructive, bringing together fields of opposite sign, which are then annihilated by diffusion.

For all our computations we take, say,

$$\begin{aligned} \psi &= \sqrt{1.5} [\cos(x + \cos t) + \sin(y + \sin t)] \\ &= \sqrt{1.5} f(x, y, t), \end{aligned} \quad (6)$$

We have chosen to focus on this particular form of ψ as it is a flow that has already received some attention and one whose chaotic properties are well documented [5,7,8]. However, there is nothing intrinsically special about this form of ψ ; it is simply one member of a family of flows that act as fast dynamos [9].

We consider three different forms for w . First (flow V1) we take $w = \psi$, as in Ref. [5,7]; the flow is then maximally helical with $h = -|\mathbf{u}|^2$. For our second flow (V2) we take $w = \sqrt{1.2}(f^2 - 1)$, where the multiplicative constant is chosen to ensure that the energy is the same as that of flow V1; this flow (which has zero mean velocity) has non-vanishing h (except at isolated points) but zero \mathcal{H} . For our third flow (V3) we seek a form of w such that $h \equiv 0$ (and also, trivially, $\mathcal{H} = 0$). Setting $h = 0$ leads to the first-order PDE

$$\psi_x w_x + \psi_y w_y = w \nabla^2 \psi, \quad (7)$$

which, for ψ of the form (6), has the general solution

$$w = \sin X \cos Y$$

$$\times \mathcal{F}((\cosec X - \cot X)(\sec Y + \tan Y)), \quad (8)$$

for arbitrary functions \mathcal{F} , where $X = x + \cos t$ and $Y = y + \sin t$. The simplest form is obviously to take $\mathcal{F} \equiv \text{const.}$ (thus giving a flow free of singularities) which we take to have the value $\sqrt{6}$ so as to have the same kinetic energy as the other two flows.

We have solved (1) numerically for each of the three flows described above, for a range of R_m . At any given R_m the growth rate is maximised for a certain value of k ; at large R_m this value, which is $O(1)$, becomes virtually independent of R_m . For flow V1, following Ref. [5], we take $k = 0.57$. For flows V2 and V3 the optimal values are found to be $k = 0.58$, essentially the same as for flow V1, and $k = 1.4$ respectively. Fig. 1 plots the growth rate of the magnetic

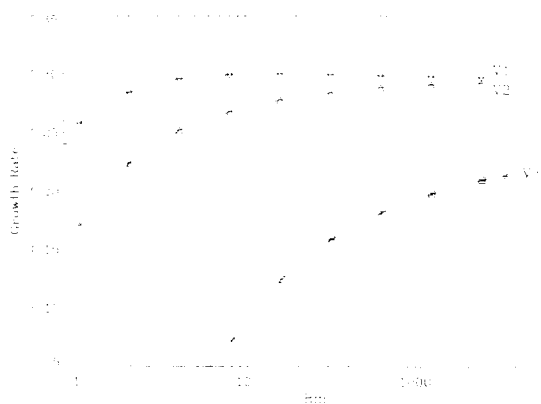


Fig. 1. Dynamo growth rates for the three flows calculated by fitting an exponential over long time traces of $\langle B \rangle^2$.

Table 1

Growth rate σ evaluated at $R_m = 2560$ for $V1$ and $V2$ and at $R_m = 3620$ for $V3$; γ_1 is defined by $\mathcal{H}_t \sim R_m^{-\gamma_1}$, γ_2 by $l_B \sim R_m^{-\gamma_2}$ and γ_3 by $l_A \sim R_m^{-\gamma_3}$.

Flow	σ	κ	D_2	γ_1	γ_2	γ_3
$V1$	0.297	0.12	1.58	0.69	0.49	0.16
$V2$	0.293	0.17	1.61	0.62	0.44	0.17
$V3$	0.214	0.25	1.58	–	0.46	0.19

field versus R_m for the three flows; the values are contained in Table 1. Flow $V1$ reaches its asymptotic state for $R_m \approx 100$, with very little variation in the growth rate as R_m is increased beyond this value. The growth rate of the field for flow $V2$ settles down at somewhat larger R_m but again provides convincing evidence of fast dynamo action. Flow $V3$, with no helicity density, is certainly a more sluggish dynamo and, with the chosen k , does not even act as a dynamo for $R_m \lesssim 40$. (Flow $V3$ *does* act as a dynamo for small values of R_m , but only for smaller values of k .) Consequently the asymptotic regime is not attained until higher values of R_m (compared to flows $V1$ and $V2$) and the evidence for fast dynamo action, although suggestive, is less compelling than that for the other two flows.

Given that all three flows have identical chaotic properties it is of interest to enquire as to how the resulting magnetic fields differ. Fig. 2 shows the magnetic helicity density h_B of the eigenfunctions at the same epoch for the three different flows. The large

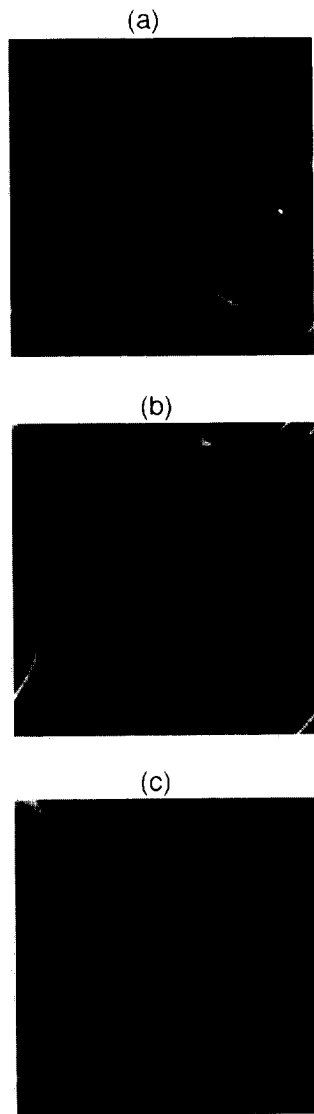


Fig. 2. Plots of the magnetic helicity density on the plane $z = 0$ at the same instant.

scale structure results from the exponential stretching in the x - y plane and hence is the same for all three flows. The influence of w can be seen in the variations in the small scale structure – this is most noticeable in the magnetic field generated by flow $V3$. Other signed measures of the magnetic field (such as the current density) yield the same qualitative picture.

The rapid changes in sign of a complicated magnetic field, as $R_m \rightarrow \infty$, can be quantified by means of the *cancellation exponent*, κ [10]. The idea of the cancellation exponent is most clearly seen by considering a scalar function of x , $q(x)$ say. Suppose the range of interest on the x -axis is covered by disjoint intervals of equal length ϵ , and then define

$$\chi(\epsilon) = \sum_i \left| \int_{\epsilon_i} q(x) dx \right|, \quad (9)$$

where ϵ_i is the i th interval of size ϵ . Then κ is defined by the scaling law

$$\chi(\epsilon) \sim \epsilon^\kappa \quad \text{as } \epsilon \rightarrow 0. \quad (10)$$

There are natural extensions of this definition to higher dimensions, where $\chi(\epsilon)$ is related to the signed flux through a plane (see Ref. [11]). For most physically relevant cases sign changes occur on scales down to some diffusive cutoff δ , below which the function becomes smooth. Definition (10) is then interpreted as applying to scales larger than δ . In such cases κ also expresses a relation between the ratio of the unsigned flux F to the signed flux Φ and the diffusive cutoff δ [12,13]. Here $\delta \sim R_m^{-1/2}$ and, by using a normalised version of (9) in two dimensions, together with (10), we obtain the expression

$$R_2 = F^2/\Phi^2 \sim R_m^\kappa. \quad (11)$$

We define F as the average of the unsigned flux of $\hat{\mathbf{B}}$ on the planes $z = 0$ and $z = \pi/k$ and Φ^2 as the average of the squares of the unsigned fluxes of $\hat{\mathbf{B}}_1$ and $\hat{\mathbf{B}}_2$ ($\hat{\mathbf{B}} = (\hat{\mathbf{B}}_1, \hat{\mathbf{B}}_2, \hat{\mathbf{B}}_3)$) on the planes $z = 0$ and $z = \pi/k$. In comparison with expressions (9) and (10), relation (11) provides an alternative means of evaluating κ in terms of more easily measurable quantities [7].

Fig. 3 shows R_2 as a function of R_m for all three flows. Since R_2 is an oscillating quantity each data point is computed as a time average over many flow periods, where the range of the oscillations is denoted by the vertical bars. The scaling relation (11) is clearly well satisfied over the entire range of R_m ; the values of κ thus computed are contained in Table 1. Clearly $\kappa(V1) < \kappa(V2) < \kappa(V3)$, which is also reflected in the differences in the fine structure of the eigenfunctions.

It should be noted that, for a given ψ , all flows of the form (4) have the same stretching properties and that

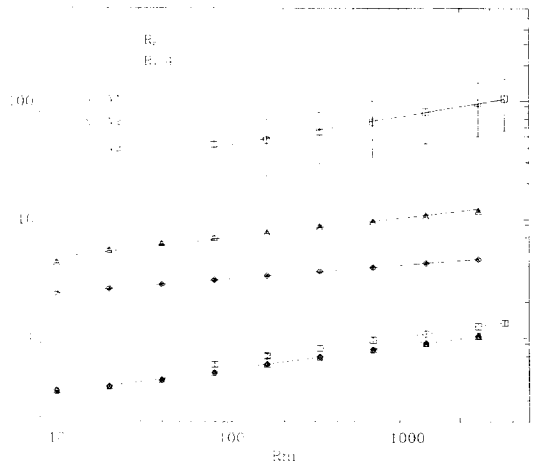


Fig. 3. Plots of R_2 and R_3 versus R_m . Each data point represents the time average over many flow periods and the vertical bars denote the amplitude of the oscillations. For all but one case the range of the oscillations is small and contained within the plotting symbols.

therefore any difference in dynamo growth rate must be due solely to differences in enhanced diffusion. The latter depends on the rate of exponential growth of gradients, as measured by the smallest Lyapunov exponents λ_3 , and on the sign changes of the magnetic field, as measured by κ . However, for all these flows λ_3 is the same and therefore the differences are due solely to differences in cancellation exponent. Thus the flow with the largest (smallest) κ gives rise to the smallest (largest) growth rate.

We now turn to the connection, if any, between the flow helicity and the magnetic helicity. For the kinematic dynamo problem the magnetic helicity \mathcal{H}_B (which is gauge invariant) grows exponentially; it is thus more convenient to work with the *relative* magnetic helicity, defined by

$$\mathcal{H}_r = \frac{\langle \mathbf{A} \cdot \mathbf{B} \rangle}{\langle A^2 \rangle^{1/2} \langle B^2 \rangle^{1/2}}, \quad (12)$$

which is a stationary quantity. The relative helicity is obviously not gauge invariant; we choose \mathbf{A} to be periodic with zero divergence and zero mean. Fig. 4 shows the variation of \mathcal{H}_r with R_m for flows $V1$ and $V2$; as before, each data point represents the time average over many periods. For flow $V3$, with zero kinetic helicity density, although \mathcal{H}_r typically is non-zero (though small) at any instant, it oscillates in sign and gives a zero time average. For flows $V1$ and $V2$, \mathcal{H}_r is pos-

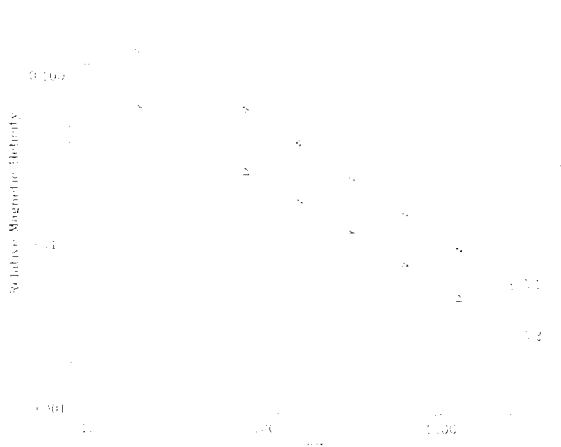


Fig. 4. Relative magnetic helicity as a function of R_m . Each data point represents the time average over many flow periods; the amplitude of the oscillations in \mathcal{H}_r is smaller than the size of the plotting symbols. \mathcal{H}_r for flow V3 is absent as it has zero time average. The values for the scaling exponents are given in Table 1.

itive and satisfies $\mathcal{H}_r(V1) > \mathcal{H}_r(V2)$, i.e. the flow with greater helicity generates a more helical magnetic field. It is of interest to note that flow V2, with no net helicity, generates an eigenfunction of positive magnetic helicity although, of course, changing the sign of w (and hence h) yields the corresponding eigenfunction with negative magnetic helicity. The most significant point to note from Fig. 4 is that \mathcal{H}_r decreases with increasing R_m , obeying a strict power law dependence. Thus the relative magnetic helicity for any fast dynamo will be vanishingly small, regardless of the helicity of the driving flow (cf. Ref. [14]). One possibility is that this is somehow related to the fact that \mathcal{H}_B is an invariant when R_m is infinite. However, this cannot explain why the relative *current* helicity, with the electric current \mathbf{J} replacing \mathbf{A} in (12), also decays with increasing R_m , even though $\langle \mathbf{J} \cdot \mathbf{B} \rangle$ is not an ideal invariant. A more likely explanation is that the result is related to the appearance of rapid fluctuations in h_B , associated with the rapid fluctuations in \mathbf{A} and \mathbf{B} as $R_m \rightarrow \infty$. To see this, we note that if the helicity density obeys a relation analogous to (11), namely

$$|\langle \mathbf{A} \cdot \mathbf{B} \rangle| / \langle |\mathbf{A} \cdot \mathbf{B}| \rangle \sim R_m^{-\alpha}, \quad (13)$$

with $\alpha \geq 0$, then the result follows trivially from the Cauchy–Schwarz inequality.

A characteristic feature of magnetic fields generated

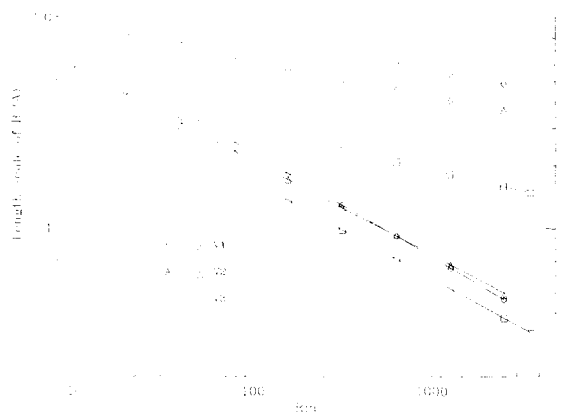


Fig. 5. Characteristic length scales of \mathbf{B} and \mathbf{A} versus R_m .

by fast dynamo action is their rapid variation on short length scales. A characteristic length scale for the magnetic field is often defined by $l_B = \langle B^2 \rangle^{1/2} / \langle J^2 \rangle^{1/2}$. Note that this quantity depends on both the local scale of \mathbf{B} and also on the filling factor. Fig. 5 shows that for all three flows the scaling law for l_B is close to $R_m^{-1/2}$. It is worth noting though that this result is more than a simple statement that diffusion sets in at such a scale – it also implies that the filling factors of \mathbf{B} and \mathbf{J} possess the same scaling with R_m as $R_m \rightarrow \infty$. The vector field \mathbf{A} , for instance, has the same $\mathcal{O}(R_m^{-1/2})$ diffusive cutoff as \mathbf{B} ; however, as can be seen from Fig. 5, the length scale of \mathbf{A} (defined by $l_A = \langle A^2 \rangle^{1/2} / \langle B^2 \rangle^{1/2}$) falls off appreciably more slowly with R_m . Care must therefore be taken when defining magnetic length scales as different measures of the field possess different scaling laws (cf. Ref. [14]).

The differences in the scaling with R_m of l_A and l_B may be attributed to the structure of the eigenfunctions at small lengthscales. Suppose that the eigenfunction of the magnetic field develops a singularity proportional to $|\mathbf{x} \cdot \mathbf{n}|^{-\alpha}$ along a line with normal \mathbf{n} and with diffusive cutoff at $|\mathbf{x} \cdot \mathbf{n}| \sim R_m^{-1/2}$. Then simple order of magnitude estimates yield

$$\langle B^2 \rangle^{1/2} \sim R_m^{(\alpha-1/2)/2} \quad (\text{provided } \alpha > 1/2), \quad (14)$$

$$\langle J^2 \rangle^{1/2} \sim R_m^{(\alpha+1/2)/2}, \quad (15)$$

$$\langle A^2 \rangle^{1/2} \sim 1 \quad (\text{provided } \alpha < 3/2). \quad (16)$$

Thus, whatever the value of α , l_B should scale as $R_m^{-1/2}$. The discrepancies in the calculated values of γ_2 for flows $V2$ and $V3$ are presumably due to not being fully in the asymptotic regime and the integrals thus picking up contributions from scales slightly larger than the diffusive cutoff. It is also easy to see that α and γ_3 are linked by the simple relation $\alpha = 2\gamma_3 + 1/2$, giving values of $\alpha = 0.82$ ($V1$), $\alpha = 0.84$ ($V2$), $\alpha = 0.88$ ($V3$). Soward [15] has stressed the importance of the singularities in the flow and has shown how, for a particular pulsed flow model, they are linked with certain fixed points of the flow. It would be of interest to try and confirm a similar relationship for the flows considered here.

The fractal dimension D_2 of the set containing most of the magnetic energy can be calculated by an expression similar to (11) [12,13,7], namely

$$R_3 = M/F^2 \sim R_m^{(D-D_2)/2}, \quad (17)$$

where M is the magnetic energy and D is the dimension of the flow in which exponential stretching occurs (equal to 2 for flows of the form (4)). In general, D_2 depends on both the stretching and cancellation properties of the flow, i.e. on λ_1 , the largest Lyapunov exponent, on λ_3 and on κ . Flows of the form (4) have the same λ_1 and λ_3 and hence differences in D_2 can arise only through differences in κ . As can be seen from Fig. 3, which plots R_3 versus R_m , the three flows yield very similar values for D_2 (given in Table 1), thus showing that for the cases we have considered the dependence of D_2 on κ is slight.

In this Letter, by focusing on three flows with identical chaotic (stretching) properties but very different helicity distributions, we have demonstrated that small scale fast dynamo action does not seem to rely crucially on the helical nature of the driving flow. Although for the flows considered here it is true that the dynamo growth rate increases with increasing helicity of the flow we believe this to be coincidental. We have argued that differences in the growth rate can derive only from differences in κ and we are unaware of any connection between the helicity of the flow and the re-

sulting cancellation exponents, these depending on the global properties of the trajectories. Concerning the helical properties of the resulting magnetic fields, our main finding is that the relative helicity for all three cases is small, vanishing as an inverse power of R_m . We believe that this is due to the development of rapid sign changes in the magnetic helicity density and, as such, the result will be true in general.

We are grateful to M. Berger, A. Gilbert, M. Proctor, A. Soward and L. Tao for helpful discussions. We particularly wish to thank S. Falle for his constant encouragement in all matters of helicity. This work was supported in part by PPARC and by the NASA Space Physics Theory Program at the University of Chicago.

References

- [1] H.K. Moffatt, Magnetic field generation in electrically conducting fluids (Cambridge Univ. Press, Cambridge 1978).
- [2] A.D. Gilbert, U. Frisch and A. Pouquet, *Geophys. Astrophys. Fluid Dyn.* 42 (1988) 151.
- [3] H.K. Moffatt, *J. Fluid Mech.* 35 (1969) 117.
- [4] V.I. Arnold, *Comptes Rendus* 261 (1965) 17.
- [5] D.J. Galloway and M.R.E. Proctor, *Nature* 356 (1992) 691.
- [6] N.F. Otani, *J. Fluid Mech.* 253 (1993) 327.
- [7] F. Cattaneo, E. Kim, M.R.E. Proctor and L. Tao, *Phys. Rev. Lett.* 75 (1995) 1522.
- [8] F. Cattaneo, D.W. Hughes and E. Kim, *Phys. Rev. Lett.* 76 (1996) 2057.
- [9] Y. Ponty, A. Pouquet and P.L. Sulem, *Geophys. Astrophys. Fluid Dyn.* 79 (1995) 239.
- [10] E. Ott, Y. Du, K.R. Sreenivasan, A. Juneja and A.K. Suri, *Phys. Rev. Lett.* 69 (1992) 2654.
- [11] Y. Du and E. Ott, *Physica D* 67 (1993) 387.
- [12] A. Bertozzi, A. Chhabra, L. Kadanoff, E. Ott and S.I. Vainshtein, unpublished.
- [13] S.I. Vainshtein, in: *Research trends in physics: Plasma Astrophysics*, La Jolla International School of Physics – Institute for Advanced Physics Studies, eds. R. Kulsrud, G. Burbridge and V. Stefan (American Institute of Physics, New York, 1994).
- [14] H.K. Moffatt and M.R.E. Proctor, *J. Fluid Mech.* 154 (1985) 493.
- [15] A.M. Soward, *Physica D* 76 (1994) 181.